Int. J. Heat Mass Transfer. Vol. 13, pp. 1925–1939. Pergamon Press 1970. Printed in Great Britain

A FUNDAMENTAL INVESTIGATION OF THE PHENOMENA THAT CHARACTERIZE LIQUID-FILM COOLING

R. A. GATER

Department of Mechanical Engineering, University of Florida, Gainesville, Florida, USA

and

M. R. L'ECUYER

Department of Mechanical Engineering, Purdue University, West Lafayette, Indiana

(*Received* 3 *September* 1969 *and in revised form* 31 *March* 1970)

Abstract— An experimental investigation was conducted to measure the net rate of mass transfer (evaporation plus entrainment) from a thin liquid film to a proximate gas stream. Also determined experimentally was the maximum film temperature and the gross characteristics of the film surface structure. Gas stream temperatures of 40°F, 400°F and 600°F, pressures of 75 psia and 150 psia, gas velocities of 40–400 fps, a film cooled length of 10 in., and film coolants of methanol, water, butanol and RP-1 were studied.

The data for mass transfer shows that the entrainment mass transfer was typically several times more important that that due to evaporation. In those cases where the evaporative mass transfer was relatively important, it is observed that the "effective" roughness of the film surface increased the evaporation by as much as 80 per cent over that predicted by the simple (or ideal) theory for mass transfer. The mass-transfer data is systematically correlated in terms of two relatively simple dimensional parameters, with one characterizing the phenomenon of entrainment and the other the phenomenon of film surface roughness.

NOMENCLATURE

B_h, blowing parameter;
C, mass concentration of vapor;
c_p, specific heat at constant pressure;
e_0, entrainment parameter;
G, $= \rho_g u_g$, gas stream mass velocity;
h, specific enthalpy;
H_v, latent heat of vaporization;
K, dimensional constant;
l_0, 10-in. long film cooled length;
l_s, scale parameter for waves of film surface;
m, rate of coolant injection or withdrawal per unit width of wetted surface;
m', rate of mass transfer from liquid film per unit width of wetted surface;
m'', local rate of mass transfer from liquid film per unit area;
M, molecular weight;
P, static pressure;
P_d, $= \rho_g u_g^2$, gas stream dynamic pressure;
P_v, partial pressure of vapor;
Pr, gas stream Prandtl number;
q'', local rate of energy transfer per unit area due to conduction;
r, roughness parameter;
Re_{x_2}, Reynolds number based on x_2;
St, Stanton number for convective heat transfer;
St', Stanton number for convective mass transfer;
T, static temperature;
u, velocity component in x direction;
We, Weber number;
x, distance measured from effective starting point of velocity boundary layer;
X_e, dimensional entrainment group;
X_r, dimensional roughness group.

Greek symbols

- μ, dynamic viscosity;
- π, dimensionless parameter defined in equation (18);
- ρ, density;
- σ, surface tension;
- ϕ, energy balance parameter.

Subscripts

- 1, evaluated at the plane of liquid injection;
- 2, evaluated at the plane of liquid withdrawal;
- c, critical;
- g, main-stream gas or state;
- l, liquid;
- L, evaluated at the gas–liquid interface in the liquid phase;
- m, maximum;
- s, simple; or evaluated at the gas–liquid interface in the gas phase;
- w, wall.

INTRODUCTION

LIQUID-FILM cooling refers to the introduction of a liquid-film onto a surface to be insulated from a proximate gas stream. Interest continues in the application of liquid-film cooling to the internal cooling problems of combustion chambers and exhaust nozzles of high-energy propulsive devices. Moreover, there is a potential application to the cooling problems of hypersonic reentry bodies.

A considerable amount of research has dealt with the basic phenomena that characterize the flow of a gas over a liquid film. For example, interfacial structure and instability [1, 2], entrainment [3, 4], wetting phenomena [5, 6], and pressure drop in annular, two-phase flow [7, 8] has been studied. However, this research has been generally characterized by experimental parameters that are significantly different from those that characterize the typical application of liquid-film cooling. It is doubtful, therefore, that the results of this research are applicable to the problem of liquid-film cooling, except in the most qualitative sense.

Research concerned specifically with the problem of liquid-film cooling has been somewhat more limited, but a number of investigations have been reported [9–12]. Unfortunately, some of the principal conclusions of these experimental investigations have been contradictory with regard to the prediction of film cooling requirements [13]. Furthermore, adequate theoretical analysis of this mass-transfer problem has been hindered by an incomplete understanding of (a) the "effective" roughness of the film surface, which should effect the convective transport, and (b) bulk entrainment of liquid caused by the breakdown of waves on the surface of the liquid-film. The research reported herein represents the first attempt to develop a meaningful mass-transfer correlation that explicitly accounts for the contributions that these interfacial phenomena make to the net rate of mass transfer.

EXPERIMENTAL

Apparatus. Figure 1 illustrates schematically the experimental apparatus employed in the investigation. The basic components of the apparatus were a hot gas generator, a two-dimensional experimental tunnel, and a variable area exhaust nozzle. The hot gas generator employed methyl alcohol and air as reactants. Because of the magnitude of diluent air added to the combustion gases before they entered the experimental tunnel, the properties of the gas stream were assumed to be the same as those for dry air.

The nominal internal dimensions of the test section were 2 in. by 5·5 in. cross section by 18 in. long. Mounted in each side wall of the test section were 6 circular Pyrex windows of 1-in. o.d. A single oblong Pyrex window was mounted in the top wall of the test section. These windows permitted visual and photographic observation of the liquid-film injected on the bottom wall of the test section. A 35 mm

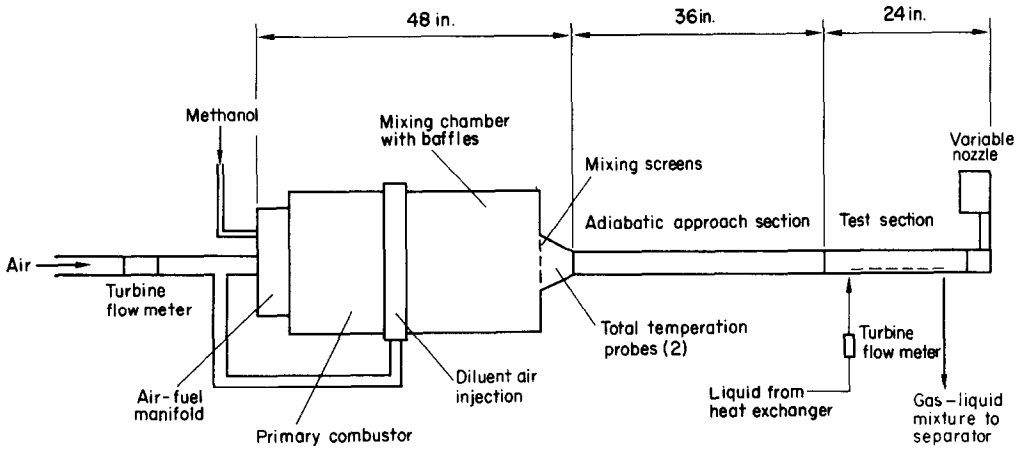

FIG. 1. Schematic diagram of experimental apparatus.

camera with a close-copy lens was employed in conjunction with a 3-μs strobe unit to photograph the film surface.

The liquid coolant was introduced onto the test plate through a flush mounted, $\frac{1}{8}$ in. thick piece of "rigimesh" that was $\frac{1}{2}$ in. long in the direction of gas flow and 2 in. wide. This injector design provided a uniform distribution of coolant and also kept the normal component of velocity for the liquid at the injector face to something less than one ft per s. The liquid film was confined to the central portion of the test plate by means of a trough machined into the plate. The trough was 2 in. wide and 0·030 in. deep, and it extended from the point of liquid injection to a point 10 in. downstream. At that point the liquid film was mechanically terminated by means of a knife-edge capture slot. The projected area of the slot for the capture of the liquid film was 2·25 in. wide by 0·060 in. high. In order to substantially reduce the lateral conduction of heat through the test plate to the liquid film, two insulating grooves (0·060 in. wide) were cut into the underside of the test plate. The grooves extended to within 0·035 in. of the surface wetted by the hot gas and were placed just outside of and parallel to the region wetted by the liquid film.

Experimental model and techniques. The experimental conditions were such that a turbulent velocity boundary layer was assumed to develop from the entrance of the experimental tunnel, $x = 0$, and the thermal boundary layer from the point of liquid injection, $x = x_1 = 40$ in. The liquid film was mechanically terminated at $x = x_2 = 50$ in., thus forming a film cooled length of 10 in. which was maintained constant throughout the investigation. The thickness of the velocity boundary layer at $x = x_1$ was on the order of 0·2–0·4 in. Calculations of displacement effects showed that the gas stream velocity generally increased by approximately five per cent in going from $x = 0$ to $x = x_1$.

The experimental technique of mechanically terminating the liquid film allowed the influence of the rate of liquid injection on the cooling process to be investigated independently of the other flow parameters. Moreover, it enabled the wetted surface area to be precisely determined so that the average rate of net mass transfer could be accurately evaluated.

Prior to injection onto the test plate, the liquid was preheated to approximately the equilibrium film temperature so as to try to realize an isothermal liquid film. This technique greatly facilitated an accurate evaluation of the physical

Table 1. Average values of the measured and calculated parameters

Test	T_g (°F)	P (psia)	u_g (fp)	G (lb/ft²s)	P_d (lb_f/ft²)	$T_{l,2}$ (°F)	$X_e \times 10^{-3}$ ($lb_f^{-\frac{1}{2}}$)	X_r ($lb_f^{\frac{1}{2}}$/ft)	m_s' (lb/s ft)
Hot flow tests									
37-W	590	78	185	37	210	190	3·87	16·4	0·00812
38-W	590	79	239	49	361	195	5·07	21·4	0·00987
39-W	601	80	288	59	523	196	6·09	26·0	0·01174
41-W	588	149	75	29	66	221	2·22	9·2	0·00584
43-W	586	155	202	81	505	232	6·09	25·2	0·01300
44-W	594	152	141	55	241	233	4·23	17·4	0·00973
45-W	650	78	430	81	1087	206	8·87	37·8	0·01682
112-M	424	75	119	27	100	129	8·16	11·1	0·01085
113-M	399	73	167	38	199	125	11·45	15·5	0·01351
114-M	402	75	247	58	445	135	17·24	23·2	0·01843
115-M	392	76	89	21	59	130	6·24	8·4	0·00791
116-M	401	73	196	45	272	134	13·59	18·1	0·01512
117-M	404	74	287	66	594	138	19·79	26·8	0·02014
118-M	609	75	221	42	286	153	14·80	19·4	0·02427
120-M	593	77	108	21	72	152	7·36	9·7	0·01340
122-M	597	74	172	33	175	144	11·38	15·2	0·01957
125-M	418	150	41	19	24	160	4·14	5·4	0·00691
126-M	404	150	86	41	109	159	8·73	11·4	0·01231
128-M	410	152	150	71	331	164	15·32	19·9	0·01965
201-B	402	77	135	32	135	190	9·33	12·6	0·01192
202-B	400	74	176	41	224	190	11·97	16·2	0·01424
203-B	400	75	52	12	20	184	3·50	4·8	0·00526
204-B	398	75	110	26	89	184	7·45	10·2	0·00987
205-B	408	76	165	39	201	190	11·23	15·4	0·01388
206-B	411	77	233	56	403	196	16·04	21·8	0·01829
207-B	400	151	56	26	45	210	5·48	7·3	0·00872
210-B	401	151	80	38	94	208	7·86	10·4	0·01205
211-B	402	151	106	50	165	206	10·54	13·8	0·01593
212-B	599	77	172	34	179	215	11·52	15·2	0·02259
213-B	595	75	126	24	94	210	8·31	11·0	0·01727
214-B	601	76	251	49	379	220	16·86	22·1	0·03054
300-R	403	76	153	36	173	280	8·46	13·9	0·00851
301-R	383	77	114	28	100	270	6·42	10·5	0·00636
302-R	400	77	194	47	285	284	10·90	17·9	0·00933
303-R	455	77	231	52	375	294	12·62	20·8	0·01489
304-R	431	152	89	41	112	290	6·84	11·3	0·01073
305-R	425	153	160	75	373	300	12·46	20·5	0·01531
306-R	642	78	112	21	75	310	5·89	9·6	0·01573
307-R	419	154	53	25	41	300	4·12	6·8	0·00615
308-R	554	77	172	35	188	338	9·04	14·9	0·01456
Cold flow tests									
47-W	20	78	69	30	65	37	1·57	8·0	—
48-W	20	78	213	93	616	32	4·85	24·6	—
102-M	42	82	35	16	17	40	2·54	4·1	—
103-M	38	78	154	66	317	34	10·90	17·6	—
104-M	40	80	90	39	108	37	6·39	10·3	—
105-M	40	77	129	53	213	34	9·00	14·5	—
109-M	26	77	181	77	434	22	12·80	20·6	—
123-M	14	75	32	13	13	28	2·17	3·5	—
124-M	14	75	147	63	287	24	10·40	16·7	—
129-M	6	73	84	36	93	32	5·86	9·4	—
215-B	10	75	150	65	300	16	10·10	17·1	—

The letter following the test number represents the liquid coolant employed: M–methanol; W–water; B—butanol; R —Rp-1.

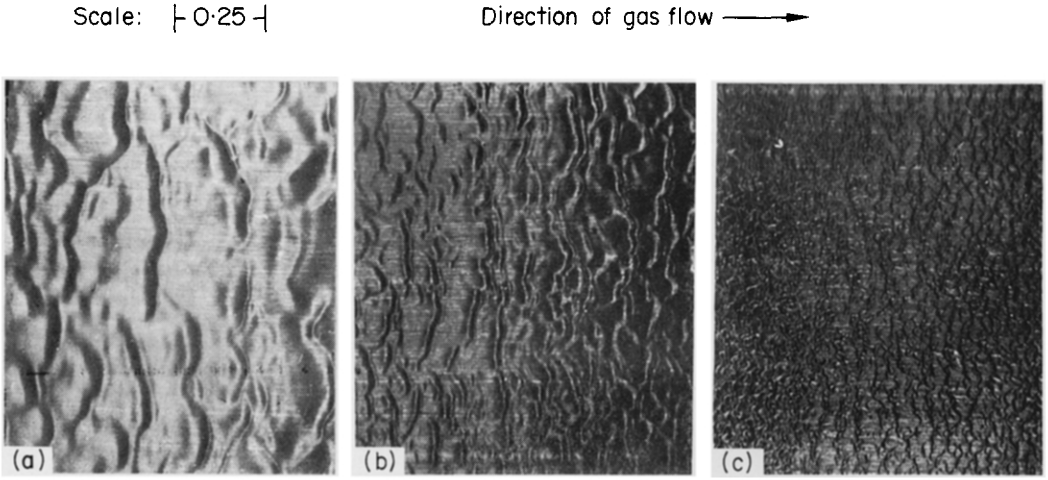

FIG. 2. Photographs of surface structure for methanol films
(a) P_d=16·8 lb$_f$/ft^2, T_g=42°F, P=82 psia.
(b) P_d=45·5 lb$_f$/ft^2, T_g=30°F, P=79 psia.
(c) P_d=172 lb$_f$/ft^2, T_g=38°F, P=77 psia.

facing page 1928

properties of the liquid film. In addition, it enabled the local energy balance at the gas–liquid interface (and not just a global energy balance) to be specified with reasonable accuracy because of the reduced variation in the sensible enthalpy of the liquid over the film cooled length.

Experimental parameters. Table 1 lists the gas stream static temperature, T_g, static pressure, P, velocity, u_g, mass velocity, $G = \rho_g u_g$, and dynamic pressure, $P_d = \rho_g u_g^2$, for the experimental tests of this report. (Tests concerned only with photographic data are not listed in Table 1.) The significance of the quantities $T_{l,2}$, X_e, X_r and m_s' in Table 1 is explained later. The coolants employed in the tests were methanol, water, butanol and RP-1 (a hydrocarbon fuel that is essentially kerosene). These experimental parameters resulted in the following variation in the pertinent physical properties for the liquid film: (a) liquid viscosity was varied by a factor of 15:1, (b) surface tension by 3:1, and (c) heat of vaporization by 4:1.

Photographic data for film surface structure. More than 200 photographs of the liquid film were studied to determine, in a qualitative sense, how the various gas stream and liquid film parameters influenced the gross film surface structure. These photographic data are studied at length in [13]. The primary conclusion of that study that is pertinent to subsequent developments herein is that the basic scale of the three-dimensional disturbance waves that develop on the film surface is principally characterized by the dynamic pressure for the gas stream, P_d, (and not G or u_g), with the scale of the waves decreasing with increasing P_d. The surface tension, σ, and the liquid viscosity, μ_l, were found to have, at most, a secondary influence on the film surface structure.

Figure 2 presents three photographs of methanol films that illustrate first the general nature of the film surface structure and then the rather considerable extent to which the gas stream dynamic pressure influences the scale of the interfacial waves. These photographs view the film normally and correspond to a location approximately 3 in. downstream from the point of liquid injection.

Data for mass transfer. Prior to making quantitative mass transfer measurements, it was necessary to insure that the liquid film was properly wetting the test surface (done visually) and that the capture slot was functioning so as to remove all of the liquid remaining on the test surface. Effective operation of the capture slot required that a certain amount of the gas phase be withdrawn with the liquid. The withdrawn two-phase mixture was separated by means of a cyclone separator with the gas phase being vented to the atmosphere and the liquid phase being collected for measurement. Figure 3

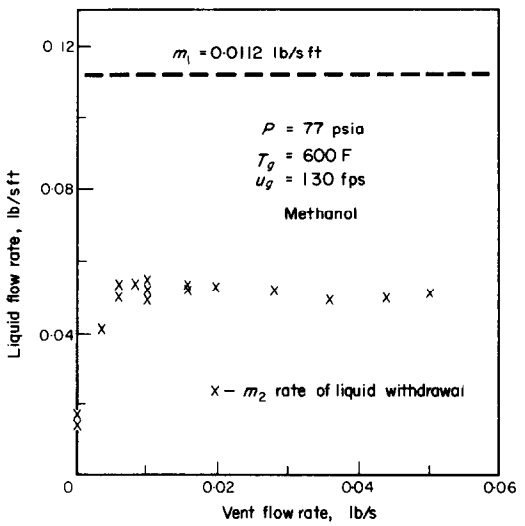

FIG. 3. Variation of liquid withdrawal rate with separator vent flow rate.

illustrates that the rate of liquid withdrawal was found to increase rapidly at first with increasing rate of vent flow from the separator and then reach a maximum, or plateau, such that a further increase in the vent flow rate did not appreciably affect the rate of liquid withdrawal. In all of the experimental tests reported herein, the vent flow rate was set equal to or greater than this limiting value. For the magnitude of vent flow rate normally required,

approximate calculations showed that the maximum amount of mass transfer that could have occurred within the separator was negligible in comparison to the total rate of mass transfer normally realized and was therefore ignored.

experimental tests, it was determined that the mass transfer due to the interfacial phenomena (surface roughness and entrainment) (a) increased linearly with the rate of liquid injection, m_1; (b) increased with decreasing values for the

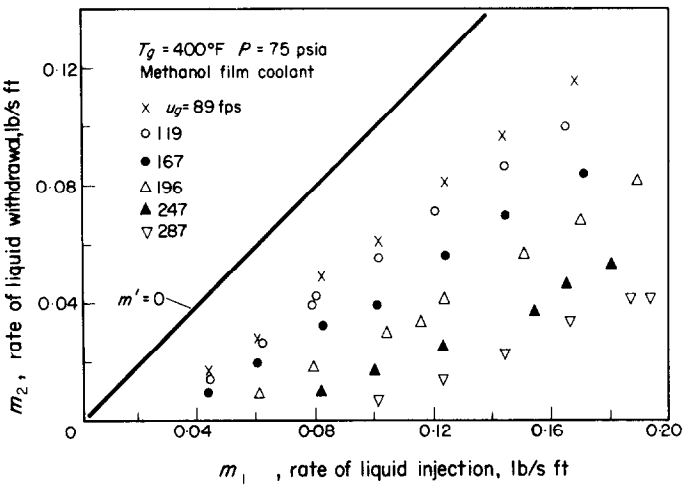

FIG. 4. Sample mass-transfer data.

Figure 4 illustrates the nature of the experimental data obtained for mass transfer. (Figure 4 gives only about 10 per cent of the data reported herein, but it is representative of all of the data.) Plotted in Fig. 4 is the rate of liquid withdrawal, m_2, as a function of the rate of liquid injection, m_1, with the gas stream velocity, u_g, as a parameter. The solid curve labeled $m' = 0$ represents the condition of no net mass transfer from the liquid film to the gas stream. The vertical distance between this solid curve and any one datum point gives the corresponding net rate of mass transfer for that datum point.

A detailed study of the experimental data was made [13] to qualitatively determine the influence of the pertinent liquid-film and gas-stream parameters on the net rate of mass transfer. First, the evaporative mass transfer predicted by the simple theory of mass transfer (as discussed below) was accounted for. Then, by simply comparing the data of all of the

surface tension σ; (c) was not a function of the viscosity of the liquid, μ_l; and (d) was characterized by the dynamic pressure for the gas stream, P_d, (and not u_g or G) with the rate of mass transfer increasing with increasing values of P_d.

Maximum film temperature. In general, the temperature of the liquid at any point within the liquid film T_l, is less than T_s, the temperature at the surface of the liquid film, and is greater than T_w, the temperature at the surface of the wetted wall. However, if the wetted surface is adiabatic, the condition $T_s \simeq T_l \simeq T_w$ is obtained when all of the energy transfer to the liquid film results in evaporation of liquid. The corresponding film temperature, which is essentially a wet-bulb temperature, is a maximum and is denoted here by $T_{l,m}$.

The temperature $T_{l,m}$ was determined experimentally by measuring $T_{l,2}$, the temperature of the liquid at the point of withdrawal. These data are presented in Fig. 5 in terms of a plot

of the measured maximum liquid temperature vs. the boiling (or saturation) temperature for the liquid at the prevailing gas stream pressure. Figure 5 illustrates that the maximum film temperature can be substantially less than the

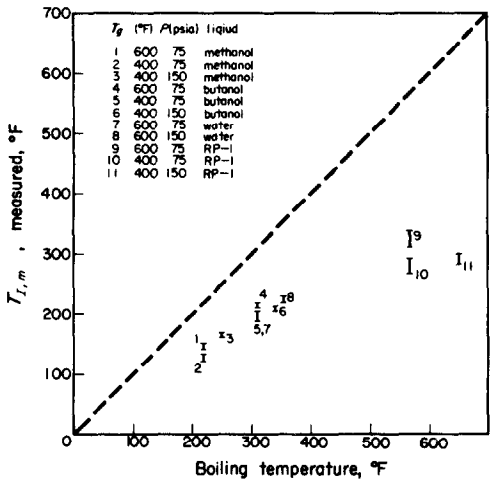

FIG. 5. Comparison of measured maximum film temperature and corresponding boiling temperature at gas stream static pressure.

boiling temperature, with the largest difference of the present investigation being approximately 355° F for RP-1 at a pressure of 150 psia and a gas stream temperature of 400 °F.

CORRELATION OF THE MASS-TRANSFER DATA

General discussion. The experimental data for mass transfer (e.g. Fig. 4) showed that, for fixed gas stream parameters, the rate of liquid withdrawal was essentially a linear function of the rate of liquid injection such that $m_2 = -A + Bm_1$. Since the quantity $(m_1 - m_2)$ is simply m', the net rate of mass transfer from the liquid film, we can write

$$m' = A + (1 - B)\, m_1. \tag{1}$$

The form of equation (1) suggests the simple hypothesis that the term A represents the evaporative contribution while the term $(1 - B)m_1$ represents the entrainment contribution to the net mass transfer. A substantial argument can, in fact, be presented to support this hypothesis [13]. However, the primary justification presented for it here is the resultant satisfactory correlation of the experimental data.

It is convenient to define a *roughness parameter*, r, so as to separate the simple evaporative mass transfer, m'_s, from that due to the effective film surface roughness:

$$A = (1 + r)\, m'_s. \tag{2}$$

In addition, it is convenient to define an *entrainment parameter*, e_0, (defined only for $l = l_0 = 10$ in.) such that

$$e_0 = 1 - B. \tag{3}$$

Doing this, equation (1) can be rewritten

$$m' = (1 + r)\, m'_s + e_0 m_1. \tag{4}$$

The parameter e_0 was determined for each experimental test from the slope of a least-squares fit of the linear relationship of m_2 and m_1 (see Fig. 4). The value of r for each condition was determined from the corresponding intercept of the linear relationship. The problem of correlating the experimental data for m' is thus reduced to that of calculating the simple mass-transfer rate m'_s and to the correlation of the parameters r and e_0 from the data.

Calculation of m'_s. Neglecting radiation heat transfer, the local rates of simple mass transfer, m''_s, and heat transfer, q''_s, are related by the interfacial energy balance

$$q''_s = q''_L + m''_s H_v \tag{5}$$

where q''_L is that portion of the total heat transfer which results in an increase in the sensible enthalpy of the liquid and/or is transferred across the wetted surface to the surroundings. Since the wetted test surface was essentially adiabatic and the liquid was preheated before injection so as to minimize the rise in sensible enthalpy of the liquid, the term q''_L is relatively small and is reasonably approximated by

$$q''_L = m''_s(h_{l,2} - h_{l,1}). \tag{6}$$

Thus, combining equations (5) and (6), we obtain from the interfacial energy balance

$$m_s'' = \frac{q_s''}{\phi} \tag{7}$$

where

$$\phi = H_v + h_{l,2} - h_{l,1}. \tag{8}$$

The net rate of simple mass transfer per unit width, m_s', is related to the local rate of simple heat transfer q_s'', through equation (7):

$$m_s' = \int_{x_1}^{x_2} \frac{q_s''}{\phi} \mathrm{d}x \simeq \frac{1}{\phi} \int_{x_1}^{x_2} q_s'' \, \mathrm{d}x. \tag{9}$$

The integral term in equation (9) was evaluated following procedures outlined in Chapters 11, 14 and 15 of the textbook by Kays [16]. Taking into account the influence of the thermal entrance length region, the variable property effects due to temperature and concentration differences, and the effect of the mass transfer, the final form of equation (9) becomes [13]:

$$m_s' = 1{\cdot}374\, l_0 G \left(\frac{T_g}{T_s}\right)^{0{\cdot}25} \left(\frac{M_s}{M_g}\right)^{0{\cdot}40} \times \ln(1 + B_h)\, St_{0{\cdot}2}. \tag{10}$$

The blowing parameter B_h can be related to the parameter ϕ by

$$B_h = \frac{c_{pg}(T_g - T_s)}{\phi}. \tag{11}$$

The reference Stanton number $St_{0{\cdot}2}$ was calculated from

$$St_{0{\cdot}2} = 0{\cdot}0295\, Pr^{-0{\cdot}4}\, Re_{x_2}^{-0{\cdot}2}. \tag{12}$$

The molecular weight, M_s, was determined from

$$\frac{1}{M_s} = \frac{C_s}{M_v} + \frac{(1 - C_s)}{M_g} \tag{13}$$

where the interfacial vapor concentration, C_s, was computed from the approximate expression

$$C_s = \frac{B_h}{1 + B_h}. \tag{14}$$

Correlation equation for e_0. A direct trial-and-error analysis of the mass transfer data showed that the entrainment parameter e_0 could be satisfactorily correlated in terms of a *dimensional entrainment group* X_e:

$$X_e \equiv \frac{P_d^{\frac{1}{2}}}{\sigma} \left(\frac{T_g}{T_s}\right)^{\frac{1}{2}} \tag{15}$$

where the temperature ratio $(T_g/T_s)^{\frac{1}{2}}$ is included to correct for variable gas density. Figure 6 presents $(1 - e_0)$ as a function of X_e, with

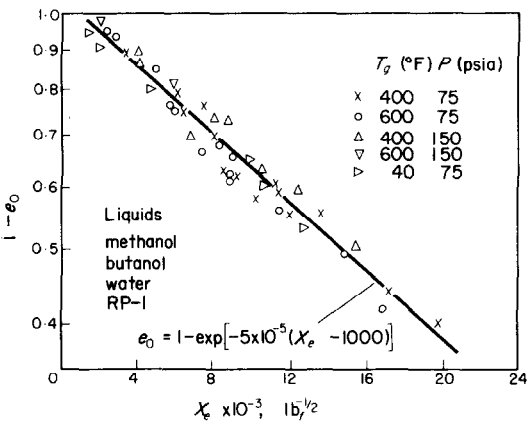

FIG. 6. Entrainment parameter e_0 as a function of entrainment group X_e.

$(1 - e_0)$ determined for each experimental test. (Recall that $1 - e_0$ is just the slope of a linear least-square fit of the mass-transfer data when presented in the form of Fig. 4.) The curve shown in Fig. 6 is given by the following correlation equation:

$$e_0 = 1{\cdot}0 - \exp[-5 \times 10^{-5}(X_e - 1000)] \tag{16}$$

where X_e is substituted with the dimensions $\mathrm{lb}_f^{-\frac{1}{2}}$. Although some scatter in the experimental data is evident, a good correlation of e_0 over the wide range investigated was obtained in terms of the relatively simple parameter X_e. Perhaps most significant is the fact that the best correlation for e_0 showed no dependence on the liquid viscosity, μ_l. This is contrary to previous proposals [11, 14] that the entrainment should

be a strong function of a Reynolds number for the film based on the liquid viscosity. [The data presented in Fig. 6 represent a variation in μ_l from $1{\cdot}7 \times 10^{-4}$ (lb_m/ft s) for water at a temperature of 265°F to 30×10^{-4} (lb_m/ft s) for butanol at a temperature of 40°F.]

Equation (16) suggests a critical value for X_e of 1000 $lb_f^{-\frac{1}{2}}$, below which negligible entrainment of liquid occurs. This result is consistent with the work of Steen and Wallis [17] who investigated in some detail the onset of entrainment from a thin liquid wall film to a proximate gas stream and suggested that a critical gas stream velocity could be defined by

$$\pi_c = 2{\cdot}5 \times 10^{-4} \tag{17}$$

where

$$\pi \equiv \frac{u_g \mu_g}{\sigma}\left(\frac{\rho_g}{\rho_l}\right)^{\frac{1}{2}} = \frac{\mu_g}{\rho_l^{\frac{1}{2}}} X_e. \tag{18}$$

Since the data reported by Steen and Wallis were for cold air flow ($T_g = T_s$) with most of the data for water as the liquid phase, substitution of representative values of μ_g and ρ_l into equation (18) gives:

$$X_e \simeq 3{\cdot}8 \times 10^6 \pi \,(lb_f^{-\frac{1}{2}}). \tag{19}$$

Thus, equations (17) and (19) give a corresponding critical value for X_e of 950 $lb_f^{-\frac{1}{2}}$, which agrees closely with the value of 1000 $lb_f^{-\frac{1}{2}}$ suggested by equation (16). It must be emphasized, however, that it was not possible to correlate the entrainment parameter e_0 in terms of π because, unlike the investigation of [17], the gas stream viscosity, μ_g, varied substantially in the present investigation. Therefore, although the parameter π is attractive in that it is dimensionless, the present data suggest that the parameter X_e better characterizes the phenomenon of entrainment.

Physical interpretation of the parameter X_e. The dimensional form of the correlation parameter X_e, obtained empirically in seeking the best correlation of the data leaves some uncertainty in assessing the physical significance of the relationship between the variables governing the phenomenon of entrainment. However, it is reasonable to expect the entrainment to be largely influenced by aerodynamic drag and surface tension forces acting on the interfacial waves. If the scale of the interfacial waves is characterized by a dimension l_s, then the ratio of the aerodynamic drag and surface tension forces acting on a wave define a dimensionless Weber number, We:

$$We \equiv \frac{P_d l_s^2}{\sigma l_s} = \frac{P_d l_s}{\sigma}. \tag{20}$$

Upon comparing the defining equations for X_e and We, [ignoring for the sake of argument the term $(T_g/T_s)^{\frac{1}{2}}$] it is seen that X_e would be proportional to We if a dimensional constant K existed such that

$$K = \frac{We}{Xe} = l_s P_d^{\frac{1}{2}} = \text{constant}. \tag{21}$$

There is, in fact, some support for the suggested inverse relationship between l_s and P_d. Recall that qualitative analysis of extensive photographic data showed that the dynamic pressure of the gas stream, P_d, (and not G or μ_g or any parameter for the liquid phase) was the parameter that most characterized the scale of the interfacial waves. Moreover, the scale was found to decrease with increasing values of P_d. Therefore, although the exponent of $\frac{1}{2}$ in equation (21) cannot be substantiated, there is some physical evidence to support the form of the equation.

Another interesting observation can be made with reference to the statement of equation (21). Shattering (or atomization) of liquid drops suspended in a gas stream is known to be characterized by a critical Weber number of about 6, where the characteristic length is chosen as the radius of the drop [18]. Drawing an analogy between the breakdown of such liquid drops and the breakdown of interfacial disturbance waves, an approximate calculation can be made for the suggested dimensional

constant K:

$$K = \frac{We_c}{X_{e,c}} \simeq \frac{6}{1000} = 0{\cdot}006\,\text{lb}_f^{\frac{1}{2}}. \quad (22)$$

Using this value for K, together with equation (21) and the data of Table 1 for P_d, we calculate a maximum and a minimum value of the scale l_s for the data of the present report of 0·00135 ft and 0·00018 ft, respectively. While these calculations are obviously very approximate, the values obtained for the scale l_s are surprisingly similar to the dimensions that characterize the structure of a liquid film subjected to relatively large interfacial shear forces [1].

In summary, it would appear possible to recast the correlation equation (16) for the entrainment parameter e_0 in terms of a dimensionless Weber number. While this procedure has some inherent advantages, it tends to obscure the fact that the dynamic pressure, P_d, and the surface tension, σ, alone were found to completely dominate the entrainment mass transfer. Hence, it is suggested that the correlation equation (16) be retained in its dimensional form.

Correlation of r. As a first approximation, it is assumed that the extent to which the interfacial structure intensified the convective transport is primarily a function of the scale parameter l_s; i.e. we assume

$$r = r(l_s). \quad (23)$$

On the basis of the foregoing interpretation of the physical significance of X_e, it follows from equation (21) that l_s can be approximately related to the square root of the dynamic pressure of the gas stream. Consequently, introducing a correction for variable gas density, a *dimensional roughness group* X_r is defined by

$$X_r \equiv P_d^{\frac{1}{2}} \left(\frac{T_g}{T_s}\right)^{\frac{1}{2}} \quad (24)$$

and equation (23) is rewritten in the form

$$r = r(X_r). \quad (25)$$

Figure 7 presents the parameter r as a function of X_r for the data of the present report. (Note that $(1 + r)\,m_s'$ is just the negative of the intercept on the abscissa of a linear fit of the data when presented in the form of Fig. 4.) Although the data in Fig. 7 exhibit considerable scatter, much

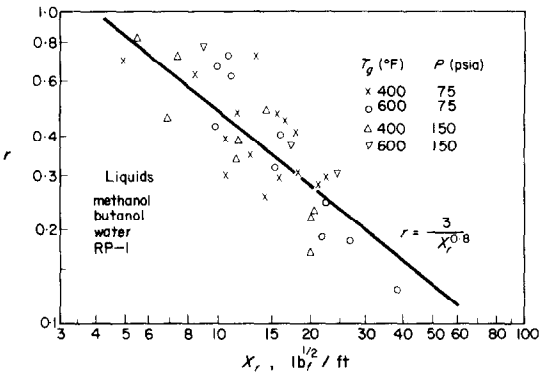

FIG. 7. Roughness parameter r as a function of roughness group X_r.

of this scatter can be attributed to the fact that the determination of r was very sensitive to experimental error in the measurement of the net rate of mass transfer [13]. However, some of the scatter in the data is no doubt due to the fact that the rather complex phenomenon of interfacial roughness cannot be characterized completely in terms of the relatively simple parameter X_r.

The curve shown in Fig. 7 is given by the expression

$$r = \frac{3{\cdot}0}{X_r^{0{\cdot}8}} \quad (26)$$

where X_r has dimensions of $\text{lb}_f^{\frac{1}{2}}$/ft. While the experimental data in Fig. 7 are in general agreement with this expression, the final form of equation (26) was arrived at by a trial-and-error computational procedure considering (a) the correlation of the experimental data of this report, (b) the correlation of the mass transfer data reported by Kinney *et al.* [9], and (c) the correlation of the experimental data for mass

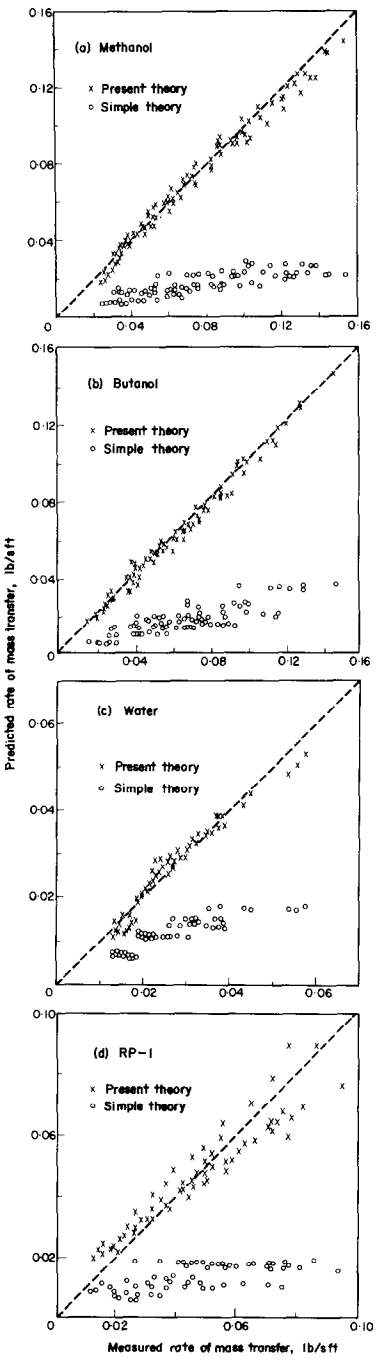

FIG. 8. Comparison of simple theory and present theory with data for mass transfer with a heated gas stream. (a) methanol, (b) butanol, (c) water, (d) RP-1.

transfer reported by Emmons and Warner [10]. It should be strongly emphasized, however, that in the analysis of both the experimental data of the present report and that of the indicated references [9] and [10], the contribution to the net mass transfer due to the effective film roughness was, with few exceptions, substantially less than the entrainment contribution. Thus, the degree of confidence in the correlation for the roughness parameter r has to be somewhat less than that for the entrainment parameter e_0.

Resultant correlation of the mass-transfer data. Figure 8 summarizes the results of the calculations for those experimental data where the gas stream was heated. The plots in Fig. 8 compare both the calculated rate of simple mass transfer and the rate of mass transfer predicted from equations (4), (16) and (26) of the present theory with the experimental data.

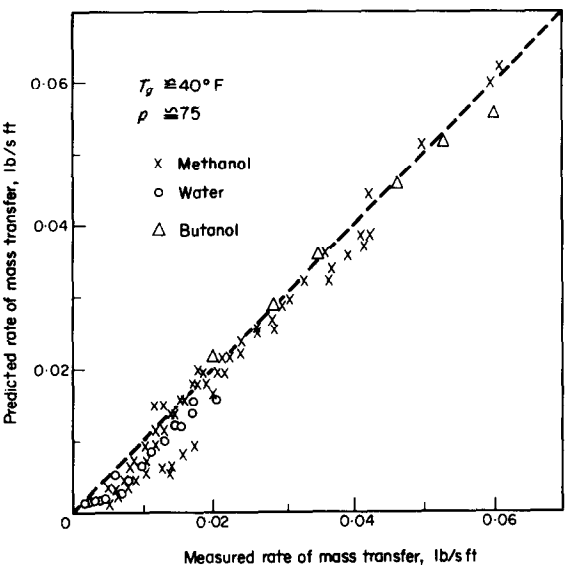

FIG. 9. Comparison of present theory with data for mass transfer with an unheated gas stream.

Figure 8 graphically demonstrates that, in general, the simple theory for mass transfer is a poor approximation to the complex phenomena that characterize liquid-film cooling. The maximum difference between the experimental data

and the result predicted from the simple theory is shown in Fig. 8(a) for methanol as the film coolant. For the measured mass-transfer rate of 0·154 (lb/sft), the corresponding calculated simple rate of mass transfer is 0·022 (lb/sft), a difference of 700 per cent. Similarly, the maximum difference between the result predicted from the present theory and the data is shown in Fig. 8(d) for RP-1 as the film coolant. For a measured rate of mass transfer of 0·0944 (lb/sft), the corresponding rate of mass transfer predicted by the present theory is 0·0765 (lb/sft), a difference of about 20 per cent.

Figure 9 presents the results of the computations for the cold-flow tests, where the realized rates of mass transfer were assumed to be due to entrainment only. The maximum value computed for the entrainment parameter e_0 was 0·32, as compared to a maximum value of 0·63 for the hot-flow tests. The agreement between the measured and the predicted rates of mass transfer is quite satisfactory, particularly in view of the fact that the pertinent physical properties for both the liquid and gas phase differed substantially between the hot-flow and cold-flow tests.

CORRELATION OF THE DATA FOR MAXIMUM FILM TEMPERATURE

The film temperature $T_{l,m}$ can be related to the thermodynamic parameters for the gas stream by specifying (a) an energy balance across the gas–liquid interface, and (b) an analogy between the rates of convective heat and mass transfer. For the case of an isothermal film on an adiabatic wall, the energy balance parameter $\phi \equiv q''/m''$ simplifies to

$$\phi = \phi_m = H_{v,m} \tag{27}$$

where $H_{v,m}$ is the heat of vaporization for the liquid at the temperature $T_{l,m}$. Moreover, the simplest analogy between convective heat and mass transfer is

$$St = St' \tag{28}$$

where St' is the Stanton number for evaporative mass transfer defined in terms of the interfacial vapor pressure $P_{v,m}$:

$$St' \equiv \frac{m''}{G} \frac{(P - P_{v,m})}{P_{v,m}} \frac{M_g}{M_v} \tag{29}$$

(It is significant to note that the validity of this analogy, unlike an analogy between momentum and heat or mass transfer, should not be necessarily affected by substantial liquid entrainment.) Combining equation (7) with equations (27)–(29) we obtain

$$\frac{(P - P_{v,m})}{P_{v,m}} \frac{M_g}{M_v} = \frac{H_{v,m}}{c_{pg}(T_g - T_{l,m})} \tag{30}$$

which relates the liquid temperature $T_{l,m}$ to the parameters P, T_g, c_{pg} and M_g for the gas stream.

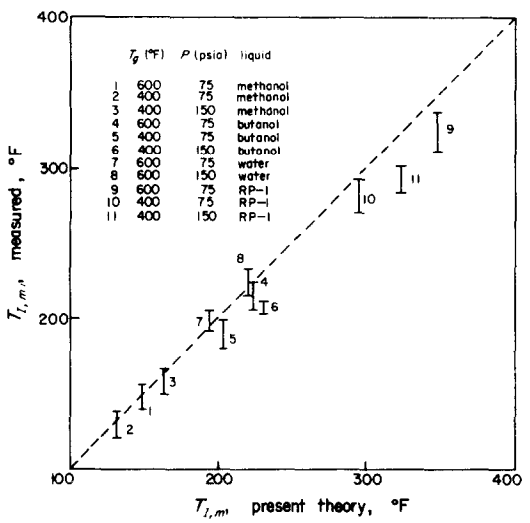

FIG. 10. Comparison of predicted maximum film temperature with measured value.

Figure 10 presents a comparison of the measured and the predicted values of $T_{l,m}$ for the data of the present report. The agreement between the experimental and analytical results shown in Fig. 10 is generally quite satisfactory, with the only substantial difference occurring for some of the data for RP-1 as the film coolant. However, the results of Fig. 10 suggest that the

simple theory is sufficiently accurate for the purposes of most engineering calculations.

CONCLUSIONS

The following principal conclusions are drawn from the results of the present investigation.

1. The scale of the interfacial disturbance waves is principally characterized by the dynamic pressure of the gas stream, P_d, with the scale decreasing with increasing values of P_d.

2. The net rate of mass transfer from a thin liquid film can be substantially greater (typically 5–10 times greater) than that predicted by the simple theory for mass transfer, with entrainment normally accounting for the bulk of the mass transfer.

3. The rate of entrainment is a function of the rate of liquid injection, m_1, the dynamic pressure, P_d, and the surface tension, σ, with the amount of liquid entrainment increasing with increasing values of m_1 and P_d and decreasing values of σ.

4. The liquid viscosity apparently does not influence the rate of entrainment, thereby contradicting the suggestion of some observers that the liquid-film Reynolds number is a primary parameter characterizing this phenomenon.

5. The "effective" roughness of the liquid film can apparently result in an increase in the evaporative mass transfer of as much as 80 per cent or more over that predicted by the simple theory.

6. The data for net mass transfer is satisfactorily correlated in terms of two dimensional parameters, with one characterizing the entrainment phenomenon and the other the phenomenon of film surface roughness. The comparison of the experimental data with the present theory shows that the agreement is generally to within 5–10 per cent.

7. There is some physical evidence that the dimensional entrainment group X_e is equivalent to a dimensionless Weber number if the characteristic length for the latter is taken as the scale of the small disturbance waves on the surface of the liquid film. Moreover, there is some evidence that the phenomenon of entrainment of liquid from the surface of a thin liquid film is analogous to the phenomenon of atomization of liquid drops suspended in a gas stream.

8. A relatively simple theory (essentially the classical theory for predicting the wet-bulb temperature) is found to predict the maximum liquid temperature with sufficient accuracy for most engineering calculations.

ACKNOWLEDGEMENTS

The investigation reported herein was initiated under the sponsorship of the Office of Naval Research, Power Branch, under Contract Nonr 1100(21). The intermediate phases of the investigation were sponsored by the National Aeronautics and Space Administration under Grant NsG 592.

The authors are indebted to Dr. B. A. Reese, Director, Jet Propulsion Center, Purdue University, for his unwavering support of the research program and for his many helpful suggestions.

REFERENCES

1. D. A. Charvonia, A study of the mean thickness of the liquid film and the characteristics of the interfacial surface in annular, two-phase flow in a vertical pipe, Report No. I-59-1, Jet Propulsion Center, Purdue University (1959).
2. A. D. Craik, Wind-generated waves in thin liquid films, *J. Fluid Mech.* **26**, 369–392 (1966).
3. S. Levy, Prediction of two-phase annular flow with liquid entrainment, *Int. J. Heat Mass Transfer* **9**, 171–188 (1966).
4. J. J. van Rossum, Experimental investigation of horizontal liquid films, *Chem. Engng Sci.* **11**, 35–52 (1959).
5. D. E. Hartley and W. Murgatroyd, Criterion for the break-up of thin liquid layers flowing isothermally over solid surfaces, *Int. J. Heat Mass Transfer* **7**, 1003–1015 (1964).
6. G. F. Hewitt and P. M. C. Lacey, The breakdown of the liquid film in annular two-phase flow, *Int. J. Heat Mass Transfer* **8**, 781–790 (1965).
7. M. Wicks and A. E. Dukler, Entrainment and pressure drop in concurrent gas–liquid flow, Part I, air–water in horizontal flow, *A.I.Ch.E. Jl* **6**, 463–468 (1960).
8. R. W. Lockhart and R. C. Martinelli, Proposed correlation of data for isothermal two-phase two component flow in pipes, *Chem. Engng Prog.* **45**, 39–48 (1949).
9. G. R. Kinney, A. E. Abramson and J. L. Sloop, Internal-liquid-film-cooling experiments with air stream temperatures to 2000°F in 2- and 4-in. diameter horizontal tubes, NACA Report 1087 (1952).

10. D. L. EMMONS and C. F. WARNER, Effects of selected gas stream flow parameters and coolant physical properties on film cooling of rocket motors, *J. Heat Transfer* **86**, 271–278 (1964).
11. E. L. KNUTH, The mechanics of film cooling–part 2, *Jet Propulsion* **25**, 16–25 (1955).
12. M. J. ZUCROW and J. P. SELLERS, JR., Experimental investigation of rocket motor film cooling, *J. Am. Rocket Soc.* **31**, 668–670 (1961).
13. R. A. GATER and M. R. L'ECUYER, A fundamental investigation of the phenomena that characterize liquid-film cooling, TM-69-1, Jet Propulsion Center, Purdue University (1969).
14. M. J. ZUCROW and A. R. GRAHAM, Some considerations of film cooling for rocket motors, *Jet Propulsion* **27**, 650–656 (1957).
15. N. HALL TAYLOR, G. F. HEWITT and P. M. C. LACEY, The motion and frequency of large disturbance waves in annular two-phase flow of air–water mixtures, *Chem. Engng Sci.* **18**, 537–552 (1963).
16. W. M. KAYS, *Convective Heat and Mass Transfer*. McGraw-Hill, New York (1966).
17. D. A. STEEN and G. B. WALLIS, The transition from annular-mist, co-current two-phase downflow, Report NYO-3114-2, Dartmouth College (1964).
18. J. G. COLLIER, and G. B. WALLIS, Two phase flow and heat transfer, Short Course Notes, Vol. 2, p. 671. Department of Mechanical Engineering, Stanford University (1967).

ÉTUDE FONDAMENTALE DES PHÉNOMÈNES QUI CARACTÉRISENT LE REFROIDISSEMENT D'UN FILM LIQUIDE

Résumé—Une étude expérimentale a été effectuée pour mesurer le flux de transfert de masse (évaporation plus entrainement) d'un mince film liquide à un courant de gaz contigu. Sont aussi déterminées la température maximale du film et les caractéristiques globales de la structure superficielle du film. On a considéré des températures de courant gazeux de 40, 400 et 600°F, des pressions de 75 psia et 150 psia, des vitesses du gaz de 40–400 fps, une longueur de film refroidi de 10 pouces et comme réfrigérants du film: méthanol, eau, butanol et RP-1. Les résultats concernant le transfert de masse montrent que le transfert de masse par entraînement est souvent plus important que celui dû à l'évaporation. Des les cas où le transfert de masse par évaporation est relativement important on observe que la rugosité effective de la surface du film augmente l'évaporation de l'ordre de 80 pour cent au-dessus de ce qui avait été prédit par la théorie simple (ou idéale) du transfert de masse. Les résultats sont systématiquement unifiés en fonction de deux paramètres dimensionnels relativement simples, avec l'un caractérisant le phénomène d'entrainement et l'autre le phénomène de rugosité superficielle du film.

EINE GRUNDSÄTZLICHE UNTERSUCHUNG DER CHARAKTERISTISCHEN PHÄNOMENE DER FLÜSSIG-FILM-KÜHLUNG

Zusammenfassung—Es wurden Versuche durchgeführt, um den gesamten Stofftransport (Verdampfung und mitgerissene Tröpfchen) von einem dünnen Flüssigkeitsfilm an einen Gasstrom zu messen. Ausserdem wurden die maximalen Filmtemperaturen und die Charakteristika der Oberflächenstruktur des Filmes experimentell bestimmt.

Die Versuche wurden bei Gastemperaturen von 4°C, 204°C und 315°C, Drücken von 5,18 bar und 10,36 bar, Gasgeschwindigkeiten von 12,2 bis 122 m/s durchgeführt. Die dem Gasstrom ausgesetzte Länge betrug 25,4 cm; als Flüssigkeiten dienten Methanol, Wasser, Butanol und RP-1.

Die Ergebnisse zeigen, dass der Stofftransport durch mitgerissene Tropfen eine mehrfach grössere Bedeutung hatte als der durch Verdampfung. In Fällen, in denen der Stofftransport durch Verdampfung einen relativ grossen Anteil hatte, wurde beobachtet, dass die "effektive Rauhigkeit" der Filmoberfläche die Verdampfung bis zu 80 Prozent über den Wert nach der einfachen (oder idealen) Theorie erhöhte. Die Versuchsergebnisse sind mit Hilfe zweier relativ einfacher Parameter systematisch zusammengefasst. Von den Parametern charakterisiert der eine das Mitreissen und der andere die "Oberflächenrauhigkeit" des Films.

ФУНДАМЕНТАЛЬНОЕ ИССЛЕДОВАНИЕ ЯВЛЕНИЙ, ХАРАКТЕРИЗУЮЩИХ ПЛЕНОЧНОЕ ОХЛАЖДЕНИЕ

Аннотация—Проведено экспериментальное исследование по измерению общей скорости переноса массы (испарение плюс унос) от тонкой пленки жидкости к прилежащему к

ней газовому потоку. Также определены экспериментально максимальная температура пленки и общие характеристики структуры поверхности пленки. Исследования проводились при следующих параметрах: температуре потока газа 40°F, 400°F, 600°F, давлении 75 псиа и 150 псиа, скоростях газа 40–400 фут/сек., длине охлаждающей пленки 10 дюймов. В качестве охладителей пленки использовались метанол, вода, бутанол и **RP**—1.

Данные по массообмену показывают, что массообмен при уносе обычно в несколько раз более важен, чем при испарении. В тех случаях, когда теплообмен при испарении играет относительно важную роль, наблюдалось, что эффективная шероховатость поверхности пленки увеличивает испарение на 80% по сравнению с испарением, предсказанным простой (идеальной) теорией массообмена. Данные по массообмену систематически обобщаются с помощью двух безразмерных параметров, характеризующих явление уноса и шероховатости пленки.